

Perspectives for coherent optical formation of strontium molecules in their electronic ground state

Christiane P. Koch*

Institut für Theoretische Physik, Freie Universität Berlin, Arnimallee 14, D-14195 Berlin, Germany

(Received 7 October 2008; published 8 December 2008)

Optical Feshbach resonances [Phys. Rev. Lett. **94**, 193001 (2005)] and pump-dump photoassociation with short laser pulses [Phys. Rev. A **73**, 033408 (2006)] have been proposed as means to coherently form stable ultracold-alkali-metal dimer molecules. In an optical Feshbach resonance, the intensity and possibly frequency of a cw laser are ramped up linearly followed by a sudden switch-off of the laser. This is applicable to tightly trapped atom pairs. In short-pulse photoassociation, the pump pulse forms a wave packet in an electronically excited state. The ensuing dynamics carries the wave packet to shorter internuclear distances where, after half a vibrational period, it can be deexcited to the electronic ground state by the dump pulse. Short-pulse photoassociation is suited for both shallow and tight traps. The applicability of these two means to produce ultracold molecules is investigated here for ^{88}Sr . Dipole-allowed transitions proceeding via the $B^1\Sigma_u^+$ excited state as well as transitions near the intercombination line are studied.

DOI: [10.1103/PhysRevA.78.063411](https://doi.org/10.1103/PhysRevA.78.063411)

PACS number(s): 32.80.Qk, 33.80.-b, 34.50.Rk, 33.90.+h

I. INTRODUCTION

The cooling and trapping of alkaline-earth metals and systems with similar electronic structure such as ytterbium have been the subject of intense research over the last decade. The interest in ultracold group-II atoms was triggered by the quest for new optical frequency standards [1]. The extremely narrow linewidth of the intercombination transition, together with the magic wavelength of an optical lattice [2], is at the heart of the clock proposals. This narrow width has several interesting implications, such as a very low Doppler temperature for laser cooling [3] or optical Feshbach resonances involving small losses and thus holding the promise of easy optical control [4–6]. Additionally ultracold alkaline-earth metals offer many more exciting perspectives: They are candidates for high-precision measurements [7,8], for studies of ultracold mixtures [9] and for the realization of quantum information processing [10,11] and quantum phases with unusual symmetries [12].

The present study focuses on strontium and addresses the question of how to produce dimer molecules in their electronic ground state from ultracold ^{88}Sr atoms. Emphasis is put on a coherent formation mechanism. Two different time-dependent schemes are studied—a ramp over an optical Feshbach resonance [13] and a sequence of short pump-dump laser pulses [14] (cf. Fig. 1)—which are both based on photoassociation resonances.

Photoassociation, the excitation of two colliding atoms into a weakly bound molecular level of an electronically excited state by laser light, has emerged as a standard tool to study the scattering properties of ultracold atoms [15]. For alkaline-earth-metal species, both dipole-allowed transitions and transitions near the intercombination line can be employed. Photoassociation based on dipole-allowed transitions near the 1S_0 - 1P_1 atomic resonance was observed for calcium [16], strontium [17,18], and ytterbium [19]. Near the narrow-

line atomic intercombination transition, photoassociation spectroscopy has been performed for strontium [20,21] and ytterbium [22].

In addition to gathering spectroscopic information, photoassociation serves as a method to produce stable ultracold molecules [23]. Depending on the properties of the electronically excited state, spontaneous decay may yield molecules in their electronic ground state [24]. However, spontaneous decay toward molecules instead of a pair of atoms occurs only if the vibrational wave functions show a large probability amplitude at short internuclear distances R . On the other hand, large free-bound Franck-Condon factors and hence very extended vibrational wave functions are required for photoassociation. Ideally the vibrational wave functions should therefore consist of both a short-range part and a long-range part. In heavy alkali-metal dimers such wave functions exist thanks to strong spin-orbit coupling [24]. In particular, the softly repulsive part of a purely long-range well [23] and resonant spin-orbit coupling [24–26] can provide the necessary “ R -transfer” mechanism. If the vibrational wave functions of the electronically excited state do not possess this dual character, molecules in the last one or two levels of the electronic ground state can be formed at most. Overwhelmingly, spontaneous decay will simply redissociate the molecules to a pair of atoms.

Photoassociation as a means to produce molecules in their electronic ground state may be more efficient if time-dependent laser fields are employed. For example, a sequence of two laser pulses, a pump pulse, and a time-delayed dump pulse can be utilized [14] [see also Fig. 1(b)]. The pump pulse excites a vibrational wave packet in the electronically excited state. The wave packet moves to shorter internuclear distances where it can be transferred to the electronic ground state by the dump pulse. The character of the vibrational wave functions decides the fate of molecule formation: The wave-packet dynamics leads to appreciable overlap with molecular levels in the electronic ground state only if the eigenfunctions from which the wave packet is built provide for it [27]. This reflects the weak-field approach

*ckoch@physik.fu-berlin.de

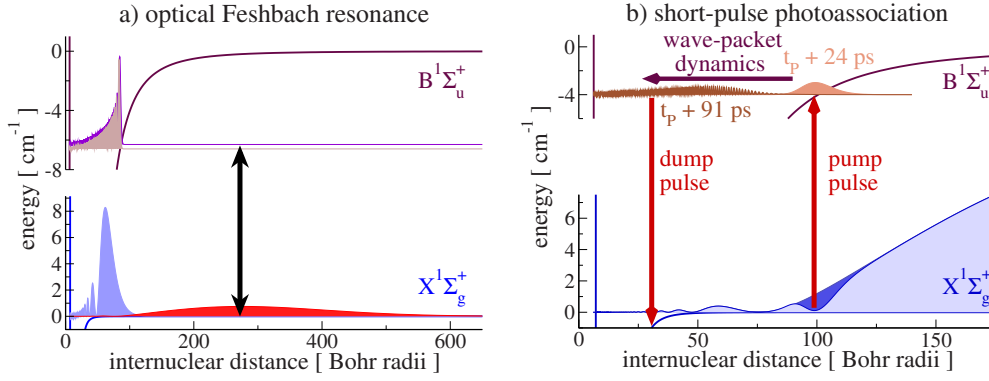


FIG. 1. (Color online) Coherent formation of ultracold strontium molecules in their electronic ground state via (a) an optical Feshbach resonance where an atom pair in the lowest state of a tight trap is adiabatically compressed to a molecule and (b) by short-pulse photoassociation where molecules are formed in a pump-dump sequence.

implicit in the pump-dump scheme where the maximum transition probabilities are completely determined by the Franck-Condon factors and the spectral amplitudes of the field.

An alternative time-dependent scheme for creating molecules in their electronic ground state consists in ramping the intensity and possibly also frequency of a continuous-wave (cw) laser over a photoassociation resonance [13] [see also Fig. 1(a)]. This has been termed optical Feshbach resonance (FR), in analogy to the formation of molecules with magnetic fields [28]. It requires an initial condition where two atoms are not too far from each other such as in a Mott insulator state of an optical lattice with two atoms per lattice site. The intensity of the laser field is ramped up slowly, while the frequency of the field is chosen such that the population of the excited state is kept minimal [13]. This ensures an adiabatic compression of the wave function while avoiding loss due to spontaneous emission. In the case of rubidium, a molecule formation efficiency of 50% was predicted for realistic laser parameters.

While the pump-dump sequence with short pulses and the ramp over an optical FR with a cw laser both represent *coherent* molecule formation schemes, they differ in a number of aspects. (i) The time scale for the pump-dump sequence is determined by the vibrational periods in the electronically excited state, which are on the order of 100 ps. Ramping over an optical FR needs to be done much more slowly, typically over 0.1–1 μ s. This time scale is set by the initial state—i.e., by the frequency of the trapping potential. (ii) Short pulses address only a small part of the initial wave function in a certain range of internuclear distances, the photoassociation window. When ramping over an optical FR, the whole wave function is adiabatically deformed.

Here, the two schemes are applied to the formation of strontium dimers in their electronic ground state. They are schematically depicted for optically allowed transitions proceeding via the Sr_2 $B^1\Sigma_u^+$ excited state in Fig. 1. Whether coherent molecule formation by optical transitions near the intercombination is possible is also studied. Similarities and

differences between alkali-metal and alkaline-earth-metal dimers are analyzed by comparing $^{88}\text{Sr}_2$ to $^{87}\text{Rb}_2$. The paper is organized as follows. Section II outlines the two-state model that is required to describe molecule formation by optically allowed transitions as well as the three-state model that presents a simplified, yet sufficiently accurate view of the physics near the intercombination line. The optical FRs are studied in Sec. III, short-pulse PA is discussed in Sec. IV, and Sec. V concludes.

II. MODEL

Two strontium atoms initially interacting via the electronic ground-state potential are considered. Assuming a harmonic trapping potential, the center-of-mass motion can be integrated analytically and is omitted from the description. For sufficiently low temperatures only *s*-wave encounters need to be taken into account. The electronic ground-state potential supports both bound levels and scattering states. A laser can excite an unbound atom pair via an electric dipole-allowed transition into bound molecular levels below the $^1S_0 + ^1P_1$ asymptote or via transitions near the intercombination line into bound molecular levels below the $^1S_0 + ^3P_1$ asymptote.

The Hamiltonian modeling electric dipole-allowed transitions between the $X^1\Sigma_g^+$ electronic ground state and the $B^1\Sigma_u^+$ electronically excited state is given by

$$\hat{H}^{DA}(t) = \begin{pmatrix} \hat{H}_g & \hat{\mu}E(t) \\ \mu E(t) & \hat{H}_e - \Delta_L(t) - \frac{i\hbar}{2}\Gamma \end{pmatrix}, \quad (1)$$

where the rotating-wave approximation (RWA) is invoked.

The single-channel Hamiltonians $\hat{H}_{g(e)}$ consist of the kinetic energy, the molecular potential energy curves, and the trap potential, $\hat{H}_{g(e)} = \hat{\mathbf{T}} + V_{g(e)}(\hat{\mathbf{R}}) + (-)V_{\text{tr}}(\hat{\mathbf{R}})$. The potentials $V_{g(e)}$ are schematically shown in Fig. 1; they are taken from Refs. [21] (V_g) and [17] (V_e). The trap is assumed to be harmonic,

$V_{\text{tr}}(\hat{\mathbf{R}}) = \frac{1}{2}m\omega_{\text{tr}}^2\hat{\mathbf{R}}^2$, with m denoting the reduced mass and ω_{tr} the trapping frequency.

Following Ref. [20], a three-channel Hamiltonian, again in the RWA, is used to model transitions near the intercombination line,

$$\hat{H}^{IC}(t) = \begin{pmatrix} \hat{H}_g & \hat{\mu}E(t) & 2\hat{\mu}E(t) \\ \hat{\mu}E(t) & \hat{H}_{0_u^+} + 4V_{\text{rot}}(\hat{\mathbf{R}}) - \Delta_L(t) - \frac{i\hbar}{2}\tilde{\Gamma} & -\frac{1}{2\sqrt{2}}V_{\text{rot}}(\hat{\mathbf{R}}) \\ 2\hat{\mu}E(t) & -\frac{1}{2\sqrt{2}}V_{\text{rot}}(\hat{\mathbf{R}}) & \hat{H}_{1_u} + 2V_{\text{rot}}(\hat{\mathbf{R}}) - \Delta_L(t) - \frac{i\hbar}{2}\tilde{\Gamma} \end{pmatrix}, \quad (2)$$

with the rotational couplings given in terms of $V_{\text{rot}}(\hat{\mathbf{R}}) = \frac{\hbar^2}{2\mu\hat{\mathbf{R}}^2}$. The potentials of Lennard-Jones type fitted to experimental data are found in Ref. [20].

The transition dipole operators are assumed to be independent of R and fixed at their atomic values; i.e., μ and $\tilde{\mu}$ are given in terms of the respective C_3 coefficients (cf. Table I).

The electric field amplitude is denoted by $E(t)$. In the case of the optical FR it corresponds to a linear function of time or to a constant, while a Gaussian pulse envelope is assumed for the short-pulse photoassociation. The detuning $\Delta_L(t) = \hbar[\omega_{\text{at}} - \omega_L(t)]$ becomes time dependent only in the case of the optical FR, and for simplicity, a linear time dependence of $\Delta_L(t)$ is chosen. The finite lifetime of the excited states is modeled by an exponential decay with decay rates Γ and $\tilde{\Gamma}$. This corresponds to the assumption that every excited-state molecule which undergoes spontaneous emission yields a hot-atom pair which is lost from the trap. The lifetimes corresponding to Γ and $\tilde{\Gamma}$ are listed in Table I.

The Hamiltonians are each represented on a Fourier grid employing an adaptive grid step [29–31]. Setting $E(t)=0$, the wave functions and binding energies of the vibrational levels are obtained by diagonalization. Analogously, dressed states are calculated by diagonalization for fixed values of $E(t)$ and $\Delta_L(t)$.

Coherent optical molecule formation is investigated by solving the time-dependent Schrödinger equation

$$\frac{\partial}{\partial t}|\Psi(t)\rangle = \hat{H}(t)|\Psi(t)\rangle,$$

with a Chebychev propagator [32], where $\hat{H}(t)$ corresponds to either Eq. (1) or (2). The state of the system at time t , $|\Psi(t)\rangle$, is represented on the mapped Fourier grid for each channel i , $\Psi_i(R;t) = \langle R|\Psi_i(t)\rangle$.

III. STRONTIUM MOLECULE FORMATION VIA OPTICAL FESHBACH RESONANCE

Molecule formation via an optical FR is based on the formal analogy between a photoassociation resonance and a magnetic FR. Instead of ramping the magnetic field magnitude, the intensity and detuning of a cw laser are increased in order to cross the resonance [13]. Then, in the dressed-state picture, the number of eigenstates below the ground-state dissociation limit is increased by 1. If the ramp is performed slowly enough, the lowest trap state is adiabatically connected to the dressed state just below the ground-state dissociation limit. This dressed state is an eigenstate of the Hamiltonian for the final values of field amplitude and detuning. However, the excited-state components of the state of the system are subject to decay due to spontaneous emission. Therefore the laser coupling between the ground and excited states should be switched off before significant spontaneous emission losses occur. A sudden switch-off of the coupling corresponds to a projection of the dressed state onto the eigenstates of the field-free Hamiltonian—i.e., onto the vibrational levels. If the dressed state before the switch-off has a large overlap with the last bound level of the electronic ground-state potential, molecules are formed.

The success of this scheme is determined by the value of the dressed-state projections onto the last bound level, which depends on the laser intensity and detuning, and by the time within which an adiabatic ramp can be performed. This time is constrained from above and below by the requirement of avoiding spontaneous emission loss and by the requirement of adiabaticity, respectively. Both limiting time scales are controlled by experimentally accessible parameters. The loss

TABLE I. C_3 coefficient and lifetime of strontium atoms for electronic states accessed by transitions near the intercombination line and by dipole-allowed transitions.

	Near the intercombination line	Dipole allowed
C_3	$0.0075E_H a_0^3$	$18.54E_H a_0^3$
Lifetime	21.46 μs	5.22 ns

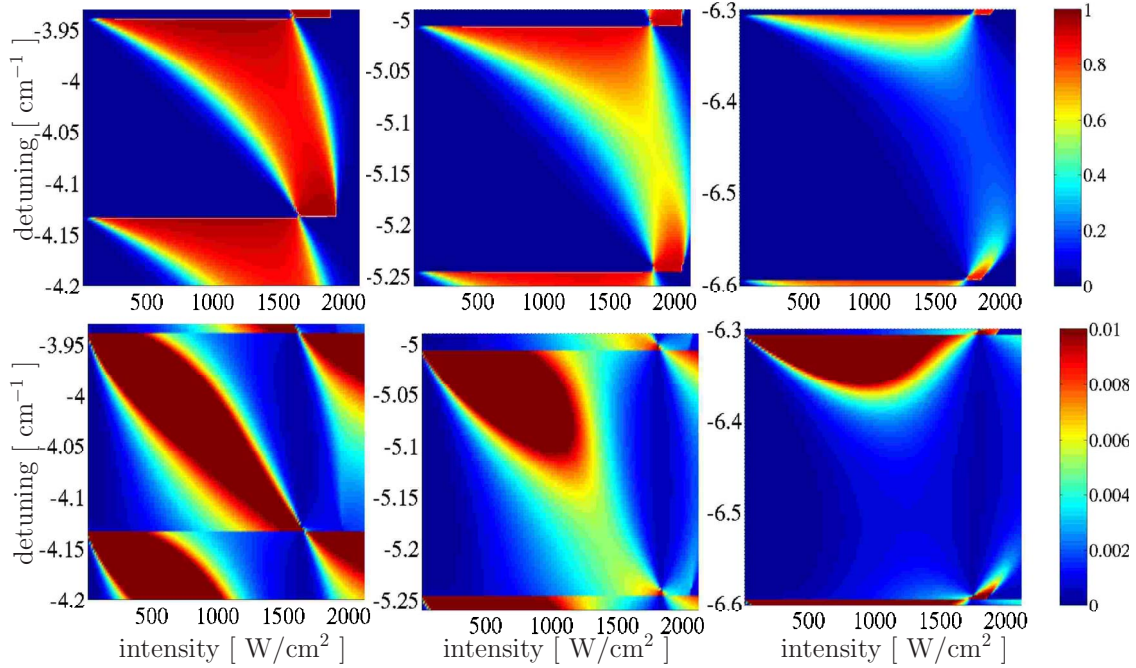


FIG. 2. (Color online) Excited-state population (bottom) and projection onto the last bound level (top) as a function of laser intensity and detuning for three different pairs of photoassociation resonances.

due to spontaneous emission depends on how much population is actually transferred to the electronically excited state—this is determined by the laser intensity and detuning. On the other hand, adiabaticity requires the ramp to be slower than the slowest internuclear dynamics—that is, slower than the vibrational period of the lowest trap state—this is determined by the trap frequency—i.e., the intensity of the trapping laser. Vibrational periods in the sub- μ s regime are realized in tight traps such as a deep optical lattice.

A. Dipole-allowed transitions $X^1\Sigma_g^+ \rightarrow B^1\Sigma_u^+$

The two quantities characterizing gain and loss in molecule formation via an optical FR—the projection of the dressed state onto the last bound level and the amount of excited-state population in the dressed state—are shown in Fig. 2 as a function of laser intensity and detuning.

When the laser detuning coincides with the binding energy of a vibrational level of the electronically excited state, large values of the projection are observed even at small laser intensity. Such a resonant transition comes at the expense of transferring a significant amount of population to the electronically excited state. Rather, detunings in between two resonances can be expected to yield large projections while keeping the population transfer to the excited state small. Note that the scale of the excited-state population is cut off at 0.01: The dark-red regions of the excited-state population should be avoided since spontaneous emission losses will be too large. Three pairs of photoassociation resonances are studied: (i) 3.938 cm^{-1} and 4.135 cm^{-1} (left column of Fig. 2), (ii) 5.006 cm^{-1} and 5.247 cm^{-1} (middle column of Fig. 2), and (iii) 6.306 cm^{-1} and 6.597 cm^{-1} (right column of Fig. 2). As the vibrational level spacing increases from left to right in Fig. 2, the areas corresponding to the

desired large projections and the undesired large excited-state populations shrink. Small regions exist at large intensity and close to the photoassociation resonance where the dressed-state projection onto the last bound level is large while the excited-state population of the dressed state is small. If the final values of field intensity and detuning correspond to such a region, the molecule formation scheme is expected to be successful. In order to determine the necessary ramps in intensity and detuning, a path needs to be identified in Fig. 2 which starts at zero intensity and leads to the target values of field intensity and detuning without passing through any of the dark-red regions with large excited-state population. A possible choice, studied below in Fig. 3, consists in ramping the intensity from zero to 1000 W/cm^2

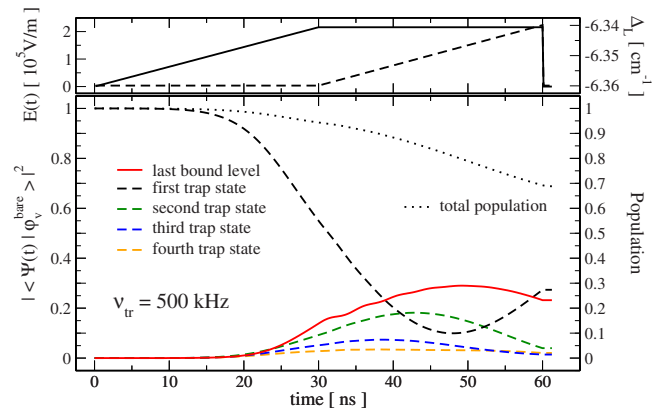


FIG. 3. (Color online) Projection of the time-dependent wave function $|\Psi(t)\rangle$ onto the last bound level and the first trap states as a function of time for a ramp of intensity followed by a ramp of frequency (bottom panel). The field amplitude (solid line) and detuning (dashed line) are shown in the upper panel.

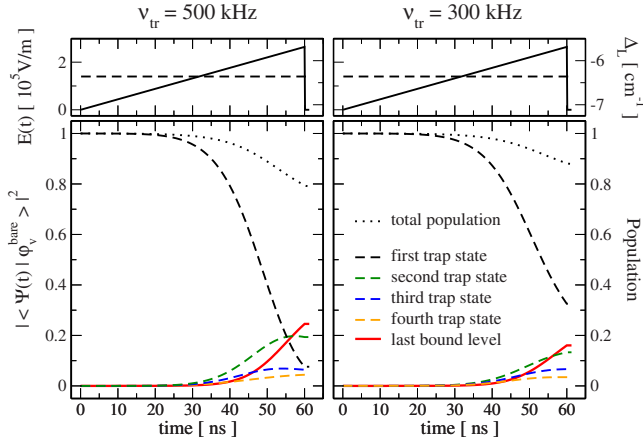


FIG. 4. (Color online) The same as in Fig. 3 for a ramp of intensity only. The detuning is kept constant at -6.36 cm^{-1} . Two different trap frequencies are compared with the adiabaticity constraint better fulfilled for the tighter trap.

at a detuning of -6.36 cm^{-1} and then ramping the detuning to -6.34 cm^{-1} (corresponding to an overall change of detuning by 600 MHz). The projection onto the last bound level of the dressed state for the final values of intensity and detuning amounts to 51%. Larger projections would require a larger final intensity and, most importantly, ramping the detuning over about 2 GHz.

Whether molecule formation in this way is feasible relies on the existence of a window of time in between the time scales set by the adiabaticity condition and by the requirement to avoid spontaneous emission. An estimate of the time scale for spontaneous emission loss is obtained by dividing the lifetime by the maximum amount of excited-state population. For laser intensities and detunings where significant overlap of the dressed state with the last bound level is achieved, the excited-state population is typically at least 1%. Given the lifetime of Sr_2 , which is by a factor of 5 shorter than that of Rb_2 , an upper limit in time of 370 ns is obtained, compared to 1.9 μs for Rb_2 [13]. This needs to be related to the vibrational period of the lowest trap state which is 29 ns (51 ns) for $\nu_{\text{tr}}=500 \text{ kHz}$ (300 kHz).

Figure 3 displays the total population together with the projections of the time-dependent wave function onto the last bound level and the first trap states as a function of time for the ramp described above.

The overall ramp time is chosen to be 60 ns. Clearly, this time is too short for the adiabaticity condition to be fully met. However, in that time, already 30% of the population is lost due to spontaneous emission (dotted line in Fig. 3). The losses occur in particular during the frequency ramp, and nonadiabatic oscillations in the time-dependent projection onto the last bound level as well as repopulation of the lowest trap state (red solid line and black dashed line in Fig. 3) are observed.

Ramps in intensity only are therefore studied in Fig. 4. The detuning is kept fixed and corresponds to that of the final detuning in Fig. 3, while the intensity is again ramped from zero to 1000 W/cm^2 .

Comparing the left-hand side of Fig. 4 to Fig. 3, the population loss is reduced to 20% and no indication of deviations

from adiabatic following are observed in the projection onto the last bound level (red solid line) and the lowest trap (black dashed line). The probability for forming molecules amounts to 25% in Fig. 4 compared to 23% in Fig. 3. Higher probabilities require larger final intensities. For example, a molecule formation probability of 33% is achieved for a final intensity of 1500 W/cm^2 (data not shown). In its left-hand and right-hand sides, Fig. 4 compares identical ramps for different trap frequencies. Adiabatic following is better enforced in the tighter trap corresponding to the faster dynamical timescale. This shows up in the smaller projection onto the last bound level and slower depletion of the lowest trap state for $\nu_{\text{tr}}=300 \text{ kHz}$ as compared to $\nu_{\text{tr}}=500 \text{ kHz}$. It is also indicated by the smaller spontaneous emission loss corresponding to less population transfer to the excited state.

Compared to Rb_2 , it is more difficult to produce ground-state molecules via an optical FR on a dipole-allowed transition in Sr_2 . The shorter excited-state lifetime of strontium requires faster ramps and leads to stronger loss of population. Only for very tight traps can adiabatic following be realized.

B. Transitions near the intercombination line

Molecule formation via an optical FR near the intercombination line turns out to be impossible. In the interpretation given above, an optical FR corresponds to an increase of the number of levels below the ground-state dissociation limit in the dressed-state picture. Generally, however, an optical FR occurs when the number of levels below the ground-state dissociation limit in the dressed-state picture is changed by 1. This number of levels could also be decreased. In that case, the usual signature of a FR—a change in the scattering length—is observed. The dressed-state wave function is, however, pushed outward to larger distances instead of being compressed inward. When crossing the resonance, the last bound molecular level becomes unbound, and obviously it is not possible to *form* molecules. This phenomenon corresponds to open-channel-dominated versus closed-channel-dominated magnetic FRs.

In the optical case, which direction a FR takes is determined by the direction of the light shift. Typically, a negative light shift corresponding to an increase in the number of bound levels is observed for $1/R^3$ long-range potentials, while $1/R^6$ long-range potentials yield a positive light shift. The potentials accessed by transitions near the intercombination line show a $1/R^3$ long-range behavior, but with a very small C_3 coefficient (cf. Table I). This leads to a curious crossover from a dipole-dipole to a van der Waals interaction—i.e., from $1/R^3$ to $1/R^6$ behavior (cf. Ref. [20] where the nine least-bound excited-state levels were measured). Only the binding energies of the last two levels correspond to the energy range where the $1/R^3$ terms of the excited-state potentials dominate the $1/R^6$ terms.

The binding energy of the dressed-state levels—i.e., the light shift—is shown as a function of intensity for the laser tuned close to the second and fourth to last levels of the excited states in Figs. 5 and 6.

The corresponding binding energies are 24.21 MHz and 353.28 MHz. Note that the binding energies are shifted by

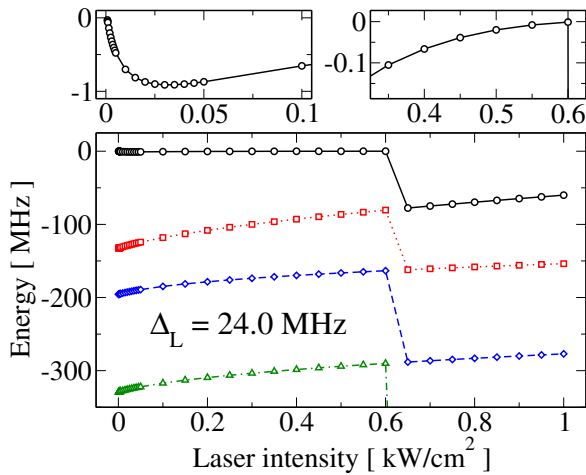


FIG. 5. (Color online) Light shift: binding energy of the least bound dressed state levels as a function of intensity for the laser tuned close to the second to last excited state level \hat{H}^{IC} (last level, black circles; second to last level, red squares; third to last level, blue diamonds; fourth to last level, green triangles). The upper panel shows the behavior of the last level near zero laser intensity and near the resonance.

the laser detunings, $\Delta_L = 24.0$ MHz in Fig. 5 and $\Delta_L = 353.0$ MHz in Fig. 6; i.e., the dressed-state representation is employed also at zero laser intensity. The binding energies appear therefore as at zero

For both photoassociation resonances, the number of dressed-state levels below the ground-state dissociation limit is decreased rather than increased: As the resonance is crossed (at about 0.6 kW/cm² in Fig. 5 and at about 160 kW/cm² in Fig. 6), the black circles are pushed above the dissociation limit and the second to last becomes the last level: The light shift is positive for both resonances. The $1/R^3$ character of the excited-state potentials shows up only at very low intensity for the resonance at 24.21 MHz; cf. the inset of Fig. 5. The binding energy of the second to last level is actually increased for laser intensities up to 0.25 kW/cm². However, at higher intensities the large positive light shift of the lower levels dominates, pushing the second to last level to smaller binding energies and finally into the scattering continuum.

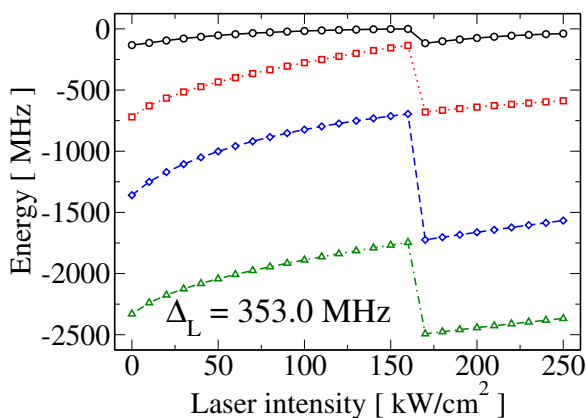


FIG. 6. (Color online) Same as Fig. 5, but for the laser tuned close to the fourth to last excited-state level of \hat{H}^{IC} .

In conclusion, a sufficiently strong $1/R^3$ long-range behavior of the excited-state potential is required to ensure a negative light shift and compression of the wave functions with increasing intensity to allow for molecule formation via an optical FR.

IV. STRONTIUM MOLECULE FORMATION VIA SHORT-PULSE PHOTOASSOCIATION

While molecule formation via an optical Feshbach resonance relies on field-free and field-dressed eigenstates and a time dependence is only invoked to adiabatically connect these eigenstates, short-pulse photoassociation is based on quantum dynamics on the much shorter time scale set by vibrational motion in the excited-state potentials. A pump-dump photoassociation scheme is employed [14,27] where the photoassociation pump pulse excites a small part of the density of colliding atoms from the electronic ground to an electronically excited state; cf. Fig. 1(b). The short-pulse duration gives rise to a finite spectral bandwidth. Population can be transferred into all excited-state vibrational levels which are resonant within the bandwidth of the pulse, and a wave packet is formed. The binding energy and spectral width of the wave packet are determined by the pump pulse detuning and bandwidth [27]. These pulse parameters need to be chosen such that excitation of the atomic transition leading to strong loss of atoms from the trap [33,34] is minimized. This requires a large enough detuning and/or small enough spectral bandwidth. At the same time, the amount of population excited into molecular levels of the excited state—i.e., the photoassociation yield—needs to be maximized. The resonance condition together with the spectral bandwidth defines a “photoassociation window” around the Condon radius [27,35]—i.e., a range of internuclear distances where population is excited. The overall amount of density of colliding atoms within this window poses an upper limit to the photoassociation yield [36]. At short internuclear distance corresponding to large detunings, the population density becomes very small. A compromise leading to a large photoassociation yield while avoiding the excitation of the atomic transition is found for detunings of a few wave numbers. In this regime, pulse energies of a few nano-joule were found sufficient to completely photoassociate all available population within the photoassociation window in the case of Rb₂ and Cs₂ molecules [27,37].

Once the excited-state wave packet is created by the photoassociation pump pulse, it oscillates back and forth on the excited-state potential. For heavy homonuclear molecules such as Rb₂ or Sr₂ and binding energies of a few wave numbers, the vibrational periods are on the order of 100 ps. Given excited-state lifetimes of nanoseconds or more, the wave packet undergoes many oscillations before it decays due to spontaneous emission. A spatial average of the wave packet would hence be observed if the deexcitation to the electronic ground state proceeds by spontaneous decay, with partial wave packets at short internuclear distance yielding molecules and those at large internuclear distance producing pairs of hot atoms. In a time-dependent approach, a second short pulse is applied when the wave packet arrives at its

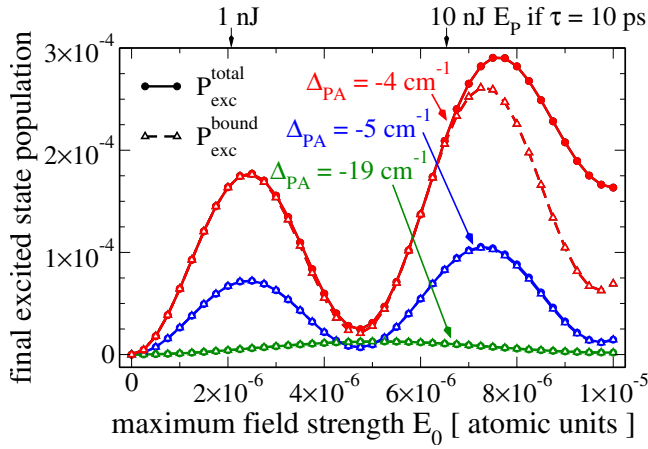


FIG. 7. (Color online) Excited-state population (solid circles) and population in bound excited-state molecular levels (open triangles) after the photoassociation pump pulse as a function of pulse energy for three different photoassociation pump pulse detunings Δ_{PA} . The populations undergo Rabi oscillations as the pulse energy is increased.

inner turning point in order to transfer a maximum amount of population to the electronic ground state; cf. Fig. 1(b). The spectral bandwidth of the dump pulse can be chosen to populate a distribution of vibrational levels or a single ground-state level [14]. The efficiency of the dump step is crucially determined by the shape of the excited-state potentials. Pure long-range potential wells with a softly repulsive part found in, e.g., the $0_g^-(P_{3/2})$ state of Cs_2 or resonantly coupled excited states such as the 0_u^+ states of Rb_2 and Cs_2 give rise to a pile-up of probability amplitude at short internuclear distances and hence to an efficient dump step [14,27].

A. Dipole allowed transitions $X^1\Sigma_g^+ \rightarrow B^1\Sigma_u^+$

The efficiency of photoassociation by the pump pulse relies on the $1/R^3$ behavior of the excited-state potential, which is almost identical for Sr_2 and Rb_2 . Similar photoassociation yields are therefore expected for Sr_2 and Rb_2 . This is confirmed by Fig. 7 (see also Table I of Ref. [27]): The final excited-state populations of Sr_2 are somewhat larger, but of the same order of magnitude as those of Rb_2 for similar pulse energies and detunings.

The slight disparity in the final excited-state populations is due to the difference in scattering lengths ($a_s \approx 2$ for ^{88}Sr [21] compared to $a_s \approx 100a_0$ for ^{87}Rb), which result in different ground-state probability densities—i.e., in differing initial conditions; cf. Fig. 1(b). In order to compare the actual numbers of P_{exc} with those obtained for Rb_2 [27], an initial state with a scattering energy corresponding to $100 \mu\text{K}$ was assumed in Fig. 7. Typically, much lower temperatures for Sr_2 are achieved by dual-stage cooling [21]. Repeating the calculation for an initial state with a scattering energy corresponding to $3 \mu\text{K}$, $\Delta_{PA} = -4 \text{ cm}^{-1}$ and $E_0 = 2.5 \times 10^{-6} \text{ a.u.}$, yields a final excited-state population which is reduced from 1.8×10^{-4} in Fig. 7 to 9.8×10^{-6} . Note that this does not necessarily imply a smaller number of molecules produced by photoassociation, since the lower temperatures come with

a higher density. The number of molecules per pulse depends on the specific configuration of the trap, in particular on the density and the number of atoms [36]. From the above considerations one can roughly estimate that at the least a similar number of molecules per pulse as for Rb_2 (on the order of 10) can be expected for Sr_2 [36].

The pulse durations in Fig. 7 were chosen to be $\tau_{\text{FWHM}} = 10 \text{ ps}$ for detunings of $\Delta_{PA} = -4 \text{ cm}^{-1}$ and $\Delta_{PA} = -5 \text{ cm}^{-1}$. The corresponding small spectral bandwidth of a 10-ps pulse, $\Delta\omega = 1.5 \text{ cm}^{-1}$, ensures that no atomic transitions are excited. For $\Delta_{PA} = -19 \text{ cm}^{-1}$, the requirement of avoiding atomic transitions is also fulfilled by shorter pulses with larger spectral bandwidth. Since the spacing between vibrational levels increases with binding energy, a larger spectral bandwidth at larger detuning allows one to address sufficiently many vibrational levels to create a wave packet. The pulse duration for $\Delta_{PA} = -19 \text{ cm}^{-1}$ was therefore taken to be $\tau_{\text{FWHM}} = 5 \text{ ps}$ (corresponding to a spectral bandwidth of $\Delta\omega = 2.9 \text{ cm}^{-1}$).

As the pulse energy is increased, Rabi oscillations in both the total excited-state population, P_{exc}^{total} , and the excited-state population in bound levels, P_{exc}^{bound} , are observed in Fig. 7. At larger detuning, the free-bound Franck-Condon factors are significantly smaller. Since the Franck-Condon factors determine the Rabi frequency, $\Omega(t) = \mu E(t)$, the largest pulse energy of Fig. 7 corresponds to a 2π pulse for $\Delta_{PA} = -19 \text{ cm}^{-1}$ compared to a 4π pulse for $\Delta_{PA} = -4 \text{ cm}^{-1}$ and $\Delta_{PA} = -5 \text{ cm}^{-1}$. At small detuning ($\Delta_{PA} = -4 \text{ cm}^{-1}$), pulse energies of 10 nJ and above lead to considerable power broadening. This is indicated in particular by the difference between the red circles and the red triangles, which corresponds to the excitation of unbound atom pairs. It emphasizes once more the necessity to avoid any spectral overlap of the field with the atomic resonance.

In a weak-field pump-dump approach, the maximum amount of population that can be transferred from the excited-state wave packet to bound ground-state levels is achieved by a π -dump pulse [14]. It is determined completely by the (time-dependent) projections of the excited-state wave packet onto the ground-state levels, $P_e^v(t) = |\langle \varphi_g^v | \Psi_e(t) \rangle|^2$. Figures 8 and 9 display the projections onto the last least-bound ground-state levels for photoassociation detunings of -4 cm^{-1} and -19 cm^{-1} .

The oscillations of the projections mirror the oscillations of the wave packet in the excited-state potential. After one vibrational period for $\Delta_{PA} = -4 \text{ cm}^{-1}$ and after four vibrational periods for $\Delta_{PA} = -19 \text{ cm}^{-1}$ the oscillations show a beat structure which is due to the wave-packet dispersion. The different vibrational periods in Figs. 8 and 9 are immediately rationalized in terms of the wave-packet binding energy—i.e., the photoassociation detuning.

At small photoassociation detuning a nonzero projection is observed for the last bound ground-state level only (Fig. 8). The wave-packet dynamics rationalizing this finding are those shown in Fig. 1(b): even when the wave packet is at its inner turning point, it is peaked at a fairly large distance, near $R = 60a_0$, and it shows a large dispersion. Clearly, such a wave packet has not got a large overlap with bound levels, and the maximum probability for transfer to the ground-state amounts to about 0.6%. Choosing a larger photoassociation

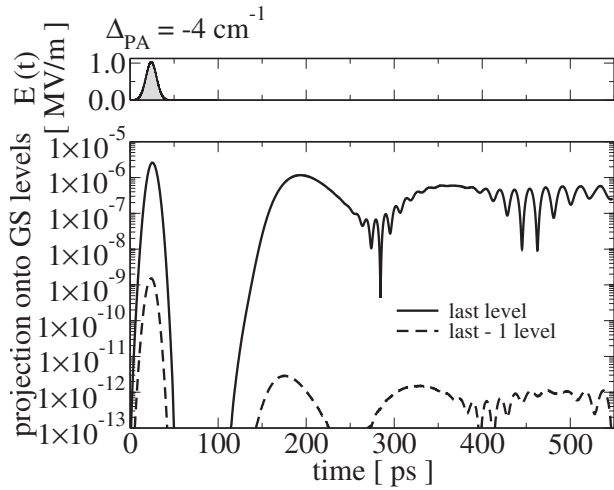


FIG. 8. Time-dependent projection of the excited-state wave packet onto ground-state vibrational levels for a photoassociation detuning of -4 cm^{-1} and a pump pulse energy of 1 nJ. The upper panel shows the photoassociation pump pulse.

detuning comes at the expense of a much smaller photoassociation excitation efficiency; cf. Fig. 7. The maximum projections seen in Fig. 9 correspond then to a transfer probability of about 15% to the last bound level and about 1% to the second to last level. Ground-state levels with substantial binding energies cannot be accessed this way.

B. Transitions near the intercombination line

The efficiency of the photoassociation pump pulse for transitions near the intercombination line is limited by the quasi- $1/R^6$ long-range behavior of the excited-state potentials. The corresponding free-bound Franck-Condon factors are several orders of magnitude smaller than for dipole-allowed transitions. While this could in principle be compensated for by employing amplified pulses with pulse energies of tens to hundreds of μJ , a further obstacle is posed by the largely reduced density of excited-state vibrational levels

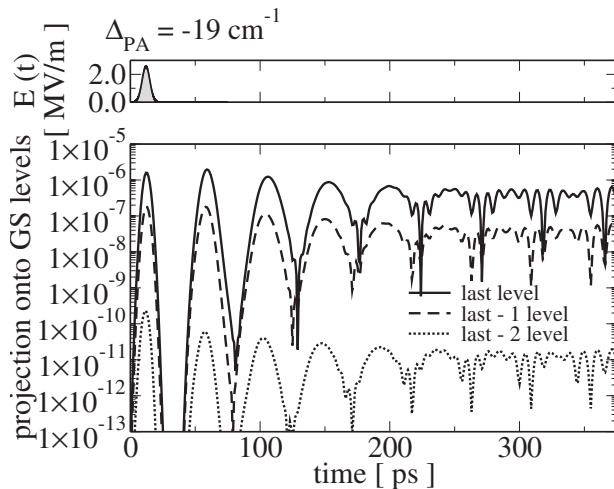


FIG. 9. Same as Fig. 8, but for a photoassociation detuning of -19 cm^{-1} and a pump pulse energy of 3 nJ.

close to the dissociation limit. Even for strong pulses, the photoassociation yield is therefore expected to be significantly smaller than the yield predicted for dipole-allowed transitions and weak pulses.

V. CONCLUSIONS

The perspectives of forming Sr_2 molecules in their electronic ground state by adiabatic ramping over an optical FR and by short-pulse photoassociation were investigated. In both schemes, molecules are formed coherently. This is unlike photoassociation with cw lasers followed by spontaneous emission [23]. Moreover, the molecule formation proceeds in a unidirectional manner for both optical FR and short-pulse photoassociations. This differs from two-photon photoassociation with cw lasers [21] where the time-reversal symmetry is not broken, creating a superposition of unbound atom pairs and molecules. While molecule formation via an optical FR is applicable in very tight traps such as deep optical lattices, short-pulse photoassociation is best adapted to shallow trapping as found in a magneto-optical trap (MOT).

Both schemes are promising when applied to optically allowed transitions proceeding via the $B \ ^1\Sigma_u^+$ excited state, and similar molecule formation rates as in Rb_2 [13,27,36] are expected. This is rationalized in terms of the similar C_3 coefficients for Sr_2 and Rb_2 . The failure of both optical FR and short-pulse photoassociations for transitions near the intercombination line is also attributed to the respective C_3 coefficient. The $1/R^3$ behavior of the relevant triplet-state potentials is caused by spin-orbit coupling and was found to be rather weak [20]. As a result, optical FRs become open-channel dominated where the atoms are pushed apart rather than pulled toward each other, and short-pulse photoassociation is inefficient due to the lack of sufficiently many bound levels close to the dissociation limit. Molecule formation by photoassociation with cw lasers followed by spontaneous emission might still be feasible. However, an estimate of the molecule formation rate based on accurate potential energy curves has yet to be given.

While coherent molecule formation via dipole-allowed transitions is predicted to be feasible, two notes of caution must be made. (i) In the case of the optical FR, a very tight trap with corresponding short vibrational period is required to allow for an adiabatic ramp over the resonance while avoiding losses due to spontaneous emission. This is due to the shorter excited-state lifetime of Sr_2 as compared to Rb_2 . (ii) In pump-dump photoassociation, the dump step is predicted to be significantly less efficient in Sr_2 than in Rb_2 . The single, deep potential well of the $\text{Sr}_2 \ B \ ^1\Sigma_u^+$ state does not facilitate a pileup of amplitude at short distance. This illustrates the difficulty of pump-dump photoassociation via a “generic” potential where no mechanism for “ R transfer” such as resonant coupling between two electronically excited states is effective.

However, deeply bound levels could be reached in Sr_2 by a pump-dump scheme if additional coherent-control techniques are employed. For example, resonant coupling can be engineered by applying an additional laser field. This has recently been suggested for short-pulse photoassociation in

Ca₂ [38]. The application of field-induced resonant coupling to strontium is beyond the scope of the present study. It is, however, expected to work for Ca₂ and Sr₂ alike due to their similar electronic structure.

A second strategy to improve photoassociation and achieve a larger number of molecules aims at increasing the photoassociation yield—i.e., the efficiency of the pump step. While Feshbach-optimized photoassociation [39] is limited to the odd isotopes of strontium, flux enhancement via coherent control of ultracold collisions [40–42] could represent a general means of pushing the atom pairs closer together before photoassociating them.

The molecule formation schemes presented here represent an important first step toward deeply bound Sr₂ molecules which are required for future high-precision measurements [8]. Once molecules in the last bound level are created, e.g.,

by ramping over an optical FR, they can be transferred toward deeply bound levels with a single strong, optimally shaped laser pulse [43], a train of weak, phase-locked pulses [44], or stimulated Raman adiabatic passage (STIRAP) [45].

ACKNOWLEDGMENTS

I would like to express my sincere gratitude to Pascal Naidon and Paul Julienne and to Philippe Pellegrini and Robin Côté for sharing the details of their respective models of the Sr₂ molecular structure. Furthermore, I am grateful to Jun Ye for drawing my attention to the alkaline-earth-metal molecules. This work was supported by the Deutsche Forschungsgemeinschaft within the Emmy Noether program (Grant No. KO 2302/1-1).

-
- [1] A. D. Ludlow, T. Zelevinsky, G. K. Campbell, S. Blatt, M. M. Boyd, M. H. G. de Miranda, M. J. Martin, J. W. Thomsen, S. M. Foreman, J. Ye *et al.*, *Science* **319**, 1805 (2008).
- [2] M. Takamoto, F.-L. Hong, R. Higashi, and H. Katori, *Nature (London)* **435**, 321 (2005).
- [3] T. Binnewies, G. Wilpers, U. Sterr, F. Riehle, J. Helmcke, T. E. Mehlstäubler, E. M. Rasel, and W. Ertmer, *Phys. Rev. Lett.* **87**, 123002 (2001).
- [4] R. Ciuryło, E. Tiesinga, and P. S. Julienne, *Phys. Rev. A* **71**, 030701(R) (2005).
- [5] R. Ciuryło, E. Tiesinga, and P. S. Julienne, *Phys. Rev. A* **74**, 022710 (2006).
- [6] P. Naidon and P. S. Julienne, *Phys. Rev. A* **74**, 062713 (2006).
- [7] G. Ferrari, N. Poli, F. Sorrentino, and G. M. Tino, *Phys. Rev. Lett.* **97**, 060402 (pages 4) (2006).
- [8] T. Zelevinsky, S. Kotochigova, and J. Ye, *Phys. Rev. Lett.* **100**, 043201 (2008).
- [9] S. Tassy, N. Nemitz, F. Baumer, C. Höhl, A. Batär, and A. Görlitz, e-print arXiv:0709.0827.
- [10] D. Hayes, P. S. Julienne, and I. H. Deutsch, *Phys. Rev. Lett.* **98**, 070501 (2007).
- [11] A. J. Daley, M. M. Boyd, J. Ye, and P. Zoller, *Phys. Rev. Lett.* **101**, 170504 (2008).
- [12] A. Hemmerich and C. M. Smith, *Phys. Rev. Lett.* **99**, 113002 (2007).
- [13] C. P. Koch, F. Masnou-Seeuws, and R. Kosloff, *Phys. Rev. Lett.* **94**, 193001 (2005).
- [14] C. P. Koch, E. Luc-Koenig, and F. Masnou-Seeuws, *Phys. Rev. A* **73**, 033408 (2006).
- [15] K. M. Jones, E. Tiesinga, P. D. Lett, and P. S. Julienne, *Rev. Mod. Phys.* **78**, 483 (2006).
- [16] G. Zinner, T. Binnewies, F. Riehle, and E. Tiemann, *Phys. Rev. Lett.* **85**, 2292 (2000).
- [17] S. B. Nagel, P. G. Mickelson, A. D. Saenz, Y. N. Martinez, Y. C. Chen, T. C. Killian, P. Pellegrini, and R. Côté, *Phys. Rev. Lett.* **94**, 083004 (2005).
- [18] P. G. Mickelson, Y. N. Martinez, A. D. Saenz, S. B. Nagel, Y. C. Chen, T. C. Killian, P. Pellegrini, and R. Côté, *Phys. Rev. Lett.* **95**, 223002 (2005).
- [19] Y. Takasu, K. Komori, K. Honda, M. Kumakura, T. Yabuzaki, and Y. Takahashi, *Phys. Rev. Lett.* **93**, 123202 (2004).
- [20] T. Zelevinsky, M. M. Boyd, A. D. Ludlow, T. Ido, J. Ye, R. Ciuryło, P. Naidon, and P. S. Julienne, *Phys. Rev. Lett.* **96**, 203201 (2006).
- [21] Y. N. Martinez de Escobar, P. G. Mickelson, P. Pellegrini, S. B. Nagel, A. Traverso, M. Yan, R. Côté, and T. C. Killian, e-print arXiv:0808.3434.
- [22] S. Tojo, M. Kitagawa, K. Enomoto, Y. Kato, Y. Takasu, M. Kumakura, and Y. Takahashi, *Phys. Rev. Lett.* **96**, 153201 (2006).
- [23] A. Fioretti, D. Comparat, A. Crubellier, O. Dulieu, F. Masnou-Seeuws, and P. Pillet, *Phys. Rev. Lett.* **80**, 4402 (1998).
- [24] C. M. Dion, C. Drag, O. Dulieu, B. Laburthe Tolra, F. Masnou-Seeuws, and P. Pillet, *Phys. Rev. Lett.* **86**, 2253 (2001).
- [25] H. K. Pechkis, D. Wang, Y. Huang, E. E. Eyler, P. L. Gould, W. C. Stwalley, and C. P. Koch, *Phys. Rev. A* **76**, 022504 (2007).
- [26] A. Fioretti, O. Dulieu, and C. Gabbanini, *J. Phys. B* **40**, 3283 (2007).
- [27] C. P. Koch, R. Kosloff, and F. Masnou-Seeuws, *Phys. Rev. A* **73**, 043409 (2006).
- [28] T. Köhler, K. Góral, and P. S. Julienne, *Rev. Mod. Phys.* **78**, 1311 (2006).
- [29] V. Kokoouline, O. Dulieu, R. Kosloff, and F. Masnou-Seeuws, *J. Chem. Phys.* **110**, 9865 (1999).
- [30] K. Willner, O. Dulieu, and F. Masnou-Seeuws, *J. Chem. Phys.* **120**, 548 (2004).
- [31] S. Kallush and R. Kosloff, *Chem. Phys. Lett.* **433**, 221 (2006).
- [32] R. Kosloff, *Annu. Rev. Phys. Chem.* **45**, 145 (1994).
- [33] W. Salzmann, U. Poschinger, R. Wester, M. Weidemüller, A. Merli, S. M. Weber, F. Sauer, M. Plewicky, F. Weise, A. Mirabal Esparza *et al.*, *Phys. Rev. A* **73**, 023414 (2006).
- [34] B. L. Brown, A. J. Dicks, and I. A. Walmsley, *Phys. Rev. Lett.* **96**, 173002 (2006).
- [35] E. Luc-Koenig, R. Kosloff, F. Masnou-Seeuws, and M. Vatasescu, *Phys. Rev. A* **70**, 033414 (2004).
- [36] C. P. Koch, R. Kosloff, E. Luc-Koenig, F. Masnou-Seeuws, and A. Crubellier, *J. Phys. B* **39**, S1017 (2006).
- [37] E. Luc-Koenig, F. Masnou-Seeuws, and M. Vatasescu, *Eur. Phys. J. D* **31**, 239 (2004).
- [38] C. P. Koch and R. Moszyński, *Phys. Rev. A* **78**, 043417 (2008).

- [39] P. Pellegrini, M. Gacesa, and R. Côté, *Phys. Rev. Lett.* **101**, 053201 (2008).
- [40] S. D. Gensemer and P. L. Gould, *Phys. Rev. Lett.* **80**, 936 (1998).
- [41] M. J. Wright, J. A. Pechkis, J. L. Carini, and P. L. Gould, *Phys. Rev. A* **74**, 063402 (2006).
- [42] M. J. Wright, J. A. Pechkis, J. L. Carini, S. Kallush, R. Kosloff, and P. L. Gould, *Phys. Rev. A* **75**, 051401(R) (2007).
- [43] C. P. Koch, J. P. Palao, R. Kosloff, and F. Masnou-Seeuws, *Phys. Rev. A* **70**, 013402 (2004).
- [44] A. Pe'er, E. A. Shapiro, M. C. Stowe, M. Shapiro, and J. Ye, *Phys. Rev. Lett.* **98**, 113004 (2007).
- [45] J. G. Danzl, E. Haller, M. Gustavsson, M. J. Mark, R. Hart, N. Bouloufa, O. Dulieu, H. Ritsch, and H.-C. Nägerl, *Science* **321**, 1062 (2008).